Appendix 1

Ministry of Science and Technology (MST), of Taiwan ***Russian Foundation for Basic Research (RFBR), Russia***

Joint Research Cooperation

■ Final
□ Progress **Report**

Project Title：Application of Rabotnov's fractional operators for the description of behavior of concrete structures during impact

Total Project Period： (2014/01/01~ 2016/12/31)

Principal Investigator (PI)：

Taiwan Side	Russia Side
(English Name) Chang Ta-Peng (Chinese Name) 張大鵬 (Position) Distinguished Professor (Department/ Institution) Department of Civil and Construction Engineering (Organization) National Taiwan University of Science and Technology (Taiwan Tech) Reference No.: (ex. 96-2923-B-00x-00y)	(English Name) Rossikhin Yuriy A. (Name in R) Россихин Юрий Алексеевич (Position) Honored Worker of Science, Professor (Department/ Institution) Scientific center for basic research in the natural sciences and construction (Organization) Voronezh State University of Architecture and Civil Engineering Reference No.:

Date of Report (yyyy/mm/dd)：2016/07/29

Appendix 2

Abstract

Nowadays, when the construction scale is substantially growing. Many of structural elements are likely subjected to impacts during their transportation, elevation, mounting, service and repair works. Sometimes the impact may cause the material microstructure damage in the contact zone and may affect its bearing properties, durability, stress-strained condition, and stress distribution of entire structure, etc. Often after the structural element is impacted there is a need to evaluate if the element can still be used. An analytical nondestructive control method for investigating the integrity of such structural elements as concrete beams impacted by a rectangular rod with a flat end was proposed by this study.

In current work the analysis of impact interaction between a Timoshenko type concrete beam and a rectangular steel rod is considered. Concrete is modeled as a viscoelastic material. Presence of the fractional parameter γ in the Rabotnov's operators allows to take into account microstructural changes of concrete with time. Because concrete aging leads to reduction of the fractional parameter γ ($0< \gamma \leq 1$); this process, in turn, causes increasing of the failure zone of the structure under the impact. Internal friction measurement using Impulse Excitation Technique allows one to determine the Elastic Storage and Loss moduli of structural member and to plot vector diagrams as main instrument in order to identify the fractional parameter of concrete and its changes with age. From beam response test the contact duration as well as maximal contact force were determined.

Theoretical model was proved by the experimental results. It was found that fractional parameter γ indeed falls into interval between 0 and 1, and is reducing with aging of concrete. Determination of contact force allowed the calculation of contact stress. Comparing the maximal contact stress with the ultimate strength of concrete, it was found that for particular conditions of the experiment the maximal contact stress was less than ultimate strength of concrete at any age. Therefore, the impact did not destroy the microstructure of the concrete beam. It was proved that the proposed analytical nondestructive control method has a good agreement between the theory and the experimental results, and can be applied to engineering practice.

Key words:
mortar beam specimen, aging of concrete, dynamic viscoelasticity, fractional operators, impact loading, nondestructive testing, acceleration

Appendix 2

Table of Contents

Appendix 2

List of Tables

List of Figures

Appendix 2

Chapter 1 Introduction

Recently, the construction industry around the world has a remarkable growth. The pace of expansion increases from an annual average of 2.7% a year in 2011-2013 to 3.1% in 2014. According to the analysis from Timetric's Construction Intelligence Center (CIC), an average annual increase of 3.9% is predicted in 2016-2020 [1].

With worldwide growth of construction area, construction risks related to accidental impacts on the structural elements obviously grow. Most of those impacts occur during the transportation, elevation, mounting, service and repair works. Some of them may cause the material microstructure changes in the contact zone and may affect its bearing properties, durability, stress-strained condition, stress distribution of entire structure etc., which, in turn creates additional risks. For safety reasons, those risks must be taken into account. A good way to estimate the damage of structures during the impact is to have a certain method to predict the behavior of the material under the impact.

The aim of this study is to analyze the concrete strength characteristics at the impact area of concrete member during its aging process under the impact. Concrete is modeled as a viscoelastic material. Presence of the fractional parameter in the Rabotnov's operators allows us to take into account the microstructural changes of concrete with time. Concrete aging leads to reduction of the fractional parameter γ ($0< \gamma \leq 1$); this process, in turn, causes increasing the failure zone of the structure under the impact.

The measurements of vector diagrams made in different ages from the concrete beams allow us to determine the time-dependent relaxed and non-relaxed moduli of concrete, as well as to define the time-dependent fractional parameter, from which the integro-differential equations of shock interaction for real concrete beams of real age can be written. By utilizing these equations, the time and initial velocity dependences of the contact force and local bearing capacity of colliding bodies can be obtained to reconstruct the picture of damage properties of concrete beams. Once the theoretical results can be well matched by the experimental data, the resulting conclusion can provide the opportunity to predict the behavior of real concrete beams at real age under the impact.

The solution to the above-mentioned problem of the concrete material subjected to impact at various ages is rather practical, since concrete structures are often subjected to the impact during their transportation, erection, maintenance, as well as during their repair or restoration. The proposed novel pioneer method of this study to solve aforementioned problems has several unique and special characteristics. First, the intricate viscoelastic models involving Rabotnov's fractional operators to describe the viscoelastic bodies behavior of concrete was adopted. Second, the changes of the microstructure of target's concrete material within the contact domain during impact was taken into account with the help of the fractional parameter. Third, the viscoelastic properties of both of the target concrete and of the impactor were considered. Fourth, the theory of discontinuities was used to describe the dynamic response of both the target and impactor being a rod with a flat end. Fifth, different from the majority of other researchers, the Poisson's ratio of concrete was considered as a

time-dependent operator, such that an intricate relationship of operators in the impact problems of concrete members were formulated and must be decoded with the help of algebra operation of the dimensionless Rabotnov's operators.

To fulfill the target of this study, the complex processes of shock interaction between the viscoelastic Timoshenko concrete beams with Rabotnov's hereditary kernel considering the effects of concrete aging and the elastic impactors have been analyzed analytically and justified by experimental work. The proposed methods which will be developed during the solution of enumerated problems could be applied to the real engineering practice for either old or newly constructed concrete structures, as well as further advanced academic studies. The theoretical investigation proposed in this study based on the application of ray method for solving the strength problems arising from the dynamic contact and shock interaction of elastic bodies considering the local microstructure has been seldom addressed before. Thus, the current study is aimed to propose a novel methodology to solve the problems involving the shock interaction of structural members made of viscoelastic concrete materials using the models involving Rabotnov's fractional-order operators to investigate aging effects of target's concrete material during the impact.

Chapter 2 Theoretical Background

Problem formulation

Let a long prismatic elastic rod of rectangular cross-section with dimensions $2\tau_{im}$ and a move along the axis z with velocity V_0 toward an isotropic rectangular Timoshenko's beam of infinite length (Fig. 2-1). The last assumption takes place because of the short impact interaction time for not considering reflected waves.

Impact occurs at the moment $t=0$ in the origin of the coordinates system x,y,z. At the moment of impact in both, in the rod and in the beam, impact waves initiated, which later propagate along the impactor and the target with velocities of transient waves.

Dynamic behavior of viscoelastic beam with consideration of rotary inertia and in-plane shear deformations can be described by the following system of equations:

$$\frac{\partial Q}{\partial z} = \rho A \dot{W}, \quad \dot{Q} = K\mu_\infty A\left[\varphi - \frac{v_\mu^\varepsilon}{\tau_\mu^\varepsilon}\int_0^t e^{-(t-t')/\tau_\mu^\varepsilon}\varphi(t')dt'\right], \tag{1}$$

$$\frac{\partial M}{\partial z} - Q = -\rho I\,\dot{\beta}, \qquad \dot{M} = -E_\infty I\left[\frac{\partial \beta}{\partial z} - \frac{v_E^\varepsilon}{\tau_E^\varepsilon}\int_0^t e^{-(t-t')/\tau_E^\varepsilon}\frac{\partial \beta(t')}{\partial z}dt'\right], \tag{2}$$

where M – bending moment, Q – lateral force, $W = \dot{w}$ - deflection rate for the points of the middle plane, β - rotation angle around z-axis of the cross-section, $\varphi = \partial w/\partial z - \beta$, v_E^ε, v_μ^ε, τ_E^ε and τ_μ^ε are the material constants, E_∞ and μ_∞ are non-relaxed values of Elastic modulus and Shear modulus, correspondingly, ρ - beam material density, K – shear coefficient, A and I are cross-section area and moment of inertia respectively, and the dot above denotes time derivative.

It is necessary to add equations describing dynamic behavior of the impactor to the equations (1) and (2):

$$\frac{\partial \sigma}{\partial z} = \rho_{im}\dot{v}, \qquad \dot{\sigma} = E_{im}\frac{\partial v}{\partial z}, \tag{3}$$

where σ - stress, v - velocity, ρ_{im} and E_{im} - impactor's material density and Yong's modulus, respectively. Also, the equation of motion for the contact area $2\tau_{im}$ in length as well as equation for the contact force F_{cont} [2] must be added (Fig. 2-1):

$$2\tau_{im}A\rho\ddot{w} = 2Q\Big|_{z=\tau_{im}} + F_{cont}, \tag{4}$$

$$F_{cont} = E_\infty(\alpha - w) - \Delta E t\int_0^t \Im_y\left(-\frac{t-t'}{\tau_\varepsilon}\right)\left[\alpha(t') - \mathrm{w(t')}\right]dt', \tag{5}$$

where α and w - displacements of upper and lower ends of the spring, respectively, displacement w equals to the beam displacement at the contact point (Fig. 2-1), τ_ε - relaxation time,

$\Delta E = E_\infty - E_0$ - defect modulus, E_0 - relaxed Yong's modulus, $\gamma (0 < \gamma \le 1)$ - fractional parameter,

$$Э_y\left(-\frac{t}{\tau_\varepsilon}\right) = \frac{t^{\gamma-1}}{\tau_\varepsilon^\gamma}\sum_{n=0}^{\infty}\frac{(-1)^n (t/\tau_\varepsilon)^{\gamma n}}{\Gamma\left[\gamma(n+1)\right]} \tag{6}$$

- Rabotnov's fractional exponential function [3], and $\Gamma(y)$ - gamma-function. Equation (6) equivalent to the standard linear solid model with fractional derivatives [4].

There is a need to add initial conditions to the system of equations:

$$\alpha\big|_{t=0} = w\big|_{t=0} = \dot{w}\big|_{t=0} = 0, \quad \dot{\alpha}\big|_{t=0} = V_0 . \tag{7}$$

Solution method

For the solution of this problem there are two methods can be used: ray method and Laplace transformation. Ray method is applicable for the construction of an approximate solution for the beam on the area from the shock wave till the border of contact area, as well as definition of exact solution in excited area of the elastic rod. Within the contact area for the contact force definition Laplace transformation is used.

In order to find solution out of the contact zone in both, the beam and the rod, compatibility condition [5]:

$$\dot{Z} = -G\frac{\partial Z}{\partial z} + \frac{\delta Z}{\delta t} \tag{8}$$

and polynomial ray expansion for the unknown functions Z, where G – normal velocity of the wave surface and $\delta Z / \delta t$ - δ-time-derivative [6,7]. As the results the following expressions for the lateral force on the border of the contact zone and contact stress in the end of the rod are obtained:

$$Q = -\rho A G_\infty W, \tag{9}$$

$$\sigma_{cont} = \rho_{im} G_{im} (V_0 - W - \dot{\alpha}), \tag{10}$$

where $G_\infty = \sqrt{K\mu_\infty / \rho}$ and $G_{im} = \sqrt{E_{im} / \rho_{im}}$ - propagation velocities of quasi-transverse shock wave and longitudinal shock wave in the rod, respectively. When the contact stress (10) is known, contact force can be found as:

$$F_{cont} = b(V_0 - W - \dot{\alpha}), \tag{11}$$

where $b = 2a\tau_{im}\rho_{im}G_{im}$.

Equations (5), (11) and (4) rewritten according to (9) in the following form

$$M\ddot{w} + MB\dot{w} = F_{cont}, \tag{12}$$

where $B = G_\infty / \tau_{im}$, and $M = 2\tau_{im} A\rho$ - mass of the contact area, represent closed system of equations with three unknowns: F_{cont}, w, α.

Applying Laplace transformation to the system of equations (5), (11) and (12), and switching

from the images to originals, using calculus of residues and the first list of Ryman's surface, the contact force can be found as

$$F_{cont}(t) = \int_0^{\infty} B(s)(1-e^{-st})ds + \frac{A}{\sqrt{k^2+\omega^2}}\left[\sin(\phi+\phi_0) - e^{-kt}\sin(\omega t+\phi+\phi_0)\right], \qquad (13)$$

where $-k \pm i\omega$ - simple poles at the first list of Riemann's surface, $tg\phi_0 = \omega / k$, and functions B(s), A and ϕ are not shown due to their bulkiness.

The first term in the expression (13) defines drift of equilibrium position, and the second one – damped vibrations around drifting equilibrium position.

Dependence of dimensionless contact force $F^*_{cont} = F_{cont}\sqrt{k^2+\omega^2} / A$ on dimensionless time $t^* = \omega t$ is shown on Fig. 2-2 for different values of the fractional parameter, which values are shown in digits near corresponding curves. Values $\gamma = 0$ and $\gamma = 1$correspond to an elastic Timoshenko beam and viscoelastic Timoshenko beam, which properties can be described by the standard linear solid model with regular viscosity.

From Fig. 2-2 it is obvious that reduction of the fractional parameter leads to reduction of both, maximum contact force and contact time.

Chapter 3 Experimental program

Study of material properties

Experimental program performed in this study is divided into two parts. The first part includes the study of material properties itself, whereas the second one is related to impact interaction between the concrete beam and the steel rod as an impactor. Since the properties of concrete mostly depend on mix proportions used in the experiments, curing conditions, etc., it is important to know the properties of all ingredients for the specific mixture to be used to cast the samples for the test. In other words, prior to the start of test, basic understanding of the material properties of all ingredients of concrete mixture must be obtained.

In this study, a batch of cylindrical concrete samples (200 mm in height and 100 mm in diameter) was cast, in which the ingredients of concrete mixture are given as: Table 3-1). Water – regular tap water.Fine and coarse aggregates: river sand and gravel, respectively (see Table 3-2). Superplasticizer – Type G superplasticizer complying with the specification of ASTM C494 [8], Yu-Lin Brand, produced in Taiwan (pH = 4.34, density = 1090 kg/m3, Cl content = 44 ppm).

The design method of ACI 211.1 mix proportions was used for the calculation of mix proportions. Water to cement ratio was 0.35. The compressive strength of concrete specimens at 28 days was designed to be around 47 MPa. Mix proportions according to ACI 211.1 method are shown in Table 3-3. The slump of fresh concrete was 50 mm as shown in Fig. 3-1, which was suitable for casting the beam specimens without the defects of honeycomb as shown in Fig. 3-2. The engineering properties of compressive strength, Dynamic Yong's Modulus, Shear Modulus, Poisson's ratio as well as Ultrasonic Pulse Velocity for concrete cylinders (200 mm in height and 100 mm in diameter) were tested. The compressive strength of concrete specimen is the capacity to withstand the axial compressive forces. When the compressive force reaches the ultimate compressive strength of concrete, the concrete cylinder crushes. The determination of compressive strength will be affected by the specific test method and the way of measurement. Thus, in this study, the test procedure complying with the requirements of ASTM C39 [9] for the compressive test of cylindrical specimens was adopted. The ASTM E1876 – 09 [10] was used to compute the dynamic elastic properties of cylindrical concrete specimens from the geometry, mass, and mechanical resonant frequencies of the concrete specimens. Dynamic Young's modulus was determined using the resonant frequency in either the flexural or longitudinal mode of vibration. The dynamic shear modulus, or modulus of rigidity, was found using the torsional resonant vibrations. Dynamic Young's modulus and dynamic shear modulus were used to compute the dynamic Poisson's ratio [10]. The Ultrasonic Pulse Velocity of cylindrical concrete specimens was measured according to ASTM C597 – 09 [11].

Impact interaction test

The main purpose of the test is to identify the contact force and contact time during the impact interaction between an elastic steel rod and a concrete beam of viscoelastic Timoshenko type and to define how these parameters are affected by aging. Three concrete beams with the rectangular cross-section of 100 mm and length of 1000 mm were cast for the impact test (see Fig. 3-2). The vibrating table was used for the fresh cylindrical concrete specimen after casting. After 24 hours, concrete specimens were demolded and stored in the lime water container. At the age of 7 days, all of the beam specimens were extracted from the water container and fixed at the experimental position as shown

in Fig. 3-3.

The schematic diagram for the experimental setup of impact test is shown in Fig. 3-4. An elastic rectangular steel rod with the cross-sectional dimension of 19.7 mm and length of 181.34 mm was used to fall down from the height of 100 mm onto a simply supported concrete beam specimen of Timoshenko type. Normally, when a simply supported beam is impacted by a relatively heavy impactor it will jump up and the resulting signal is destroyed. In order to prevent this effect, the beam must be tightly bound to the support at the ends. Such fixing method prevents both the end rotation and vertical displacements of the beam specimens at the supports.

Accelerometer of PCB 352C33 was attached to the middle of bottom surface of the beam specimen, right under the impact point to measure the acceleration of vibration of beam specimen during all the time upon the beam being hit by the impactor. The signals of acceleration obtained from the accelerometer entered into data acquisition system AD-Link and was visualized on a PC monitor using the Visual Signal software after the FFT transformation (Fig. 3-5). The software had a function to export the signal data into MS Excel file. After MS Excel data file was ready, a graphical identification of contact time could be done. It was measured manually as a difference between corresponding data points as shown in Fig. 3-6. Since the acceleration of the beam was known, the Newton's Second law was used to compute the contact force (see Fig. 3-7).

After the contact force was obtained, the contact stress could be calculated as a ratio of maximum contact force over the contact area. By comparing the contact stress with the ultimate strength, whether the local damage of the material microstructure did take place could be verified. If the contact stress did not exceed the ultimate strength of concrete, an intact condition of beam specimen was satisfied.

Internal friction test

Since in this study the concrete is assumed to be a viscoelastic material, it is important to understand the scale of viscous behavior as well as the scale for the elastic one. This ratio can be represented by the internal friction, or damping, as a ratio of the Loss Modulus over the Storage Modulus. The Storage Modulus, or the Dynamic Young's Modulus is the real part of the Complex Modulus, it represents the elastic behavior. From the other side, the Loss Modulus is the imaginary part of complex Modulus which describes the viscos behavior.

In present study, the damping was measured by the Resonant Frequency Damping Analyzer, RFDA Basic, using Impulse Excitation Technique. The details of the method were discussed in Chapter 2. Original RFDA Basic device has the following composition:

RFDA Basic software (Installation CD);

USB hardware key;

Transducer (Logitech USB-microphone);

Manual excitation device;

Reference sample;

Universal wire support;

Computer system (not included).

Three rectangular concrete beam samples (160×80×40 mm) were cast for the experiment. Mix proportions were chosen to be exactly the same as the ones for the beam specimens for the impact test. The original universal wire support (see Fig. 3-8) was not designed for concrete samples. Mass of such a specimen was between 1200 and 1300 grams, which was too heavy to be supported by the original wire, and the sample could not vibrate in proper way. Thus, to solve this problem, this study carefully designed a new steel wire support and strong steel frame, which was suitable for testing concrete samples (see Fig. 3-9). The new designed steel support had 4 steel wires with adjustable positions according to the test mode being used. Tension of wires could also be controlled by special adjusting bolts. Since it was very important for the support to be horizontal, four more adjustable bolts on the bottom surface of the support were provided. In order to verify the horizontalness of the support, two bubble level instruments were used (see Fig. 3-10). Steel wire support were able to test real concrete samples with mass over 2 kg.

Another problem related to adaptation of RFDA Basic to concrete samples tests was that the original impactor could not induce any detectable vibrations. Because of this reason the original impactor was replaced by a spherical steel impactor with diameter of 15.88 mm. In order to investigate the effect of impactor replacement on the test results, a set of preliminary experiments was conducted. Using the new steel wire support together with reference sample, four types of impactors with different sizes were used in the test:

A reference impactor of 6.30 mm in diameter;

A spherical impactor of 15.88 mm in diameter;

A spherical impactor of 9.50 mm in diameter;

A spherical impactor of 7.14 mm in diameter.

It was found that the changing of the impactor did not affect the results during the reference sample test, which can be obviously observed from the comparison of Table 3-4 to Table 3-7. By comparing the frequencies, damping values, Dynamic Elastic and Shear Moduli, Poisson's ratios, it can be noticed that corresponding values almost do not change when changing sizes of the impactor. In order to initiate detectable vibrations of the concrete sample, the steel spherical impactor 15.88 mm in diameter was selected. Experimental setup for damping test of concrete is shown in Fig. 3-11.

Vector diagram measurements and identification of the fractional parameter

When the damping and the Storage Modulus of concrete are known, the Loss Moduli can be calculated. Since $Q^{-1}=E''/E'$, therefore $E''= Q^{-1}\times E'$. By plotting the Storage Modulus vs. the frequencies, the Loss Modulus vs. frequencies, and eliminating the frequencies, the Cole-Cole diagram (E" vs. E') can be constructed. Fractional parameter is defined as a tangent slope at the beginning and at the end points of the Cole-Cole plot. Each frequency corresponds to a certain age of the sample, therefore, on the Cole-Cole diagram, the fractional parameter being taken at the first point represents the earliest age (7 days), and the value being calculated at the end point is referred to the latest age (182 days). By using these two points of the fractional parameters at 7 days and at 182 days, respectively, it is possible to draw a regression line to indicate the mean value of the results.

Laboratory equipment description

All the equipment of experimental work used in this study are listed below.

Digital Caliper “Metrology” of 300 mm in length– to measure linear dimensions of specimens with accuracy of 0.01 mm. Photos of Caliper and its Inspection Certificate presented in Fig. 3-12 and Fig. 3-13 respectively.

Electronic scale JADEVER 3016 (Fig. 3-14) with the maximum loading capacity of 30 kg and precision of 2 g.

Electronic scale Shimadzu TX4202L with the maximum loading capacity of 4200 g and precision of 0.01 g (see Fig. 3-15).

Oven of dimensions of 2.0 × 1.0 × 0.8 m having the maximum temperature of 150 ºC. with a timer to dry the fine, coarse aggregates and samples as shown in Fig. 3-16. Multi aluminum plates for drying the aggregates in the oven were used.

Grinding machine (shown in Fig. 3-17) with automatic/manual mode of supportto be selected by user. This machine was used for grinding samples in order to prepare smooth butt ends of samples before testing of compressive strength.

Concrete mixers of different capacity of big, medium and small mixers (Fig. 3-18, Fig. 3-19, Fig. 3-20 respectively).

Horizontal table for verifying the smoothness of butt ends of concrete and mortar samples (shown at Fig. 3-21).

Computer-Control Servo Hydraulic Concrete Compression Testing Machine HT-8391PC (Fig. 3-22), produced by Hung Ta Co., LTD..

Dynamic Resonant Frequency Instrument “ERUDITE” (Fig. 3-23), produced by CCNS Farnell Corporation (UK) to define the Dynamic Modulus of Elasticity and Poisson’s ratio of concrete samples via longitudinal and torsional frequencies according to ASTM C215.

Ultrasonic Pulse Velocity Meter “Pundit 7” (Fig. 3-24), produced by CNS Farnell Corporation (UK)to evaluate the quality and possible detects of irregularities inside materials by measuring travel time of ultrasonic pulses.

Vibrating table (Fig. 3-25).

Air-bubble level instruments (see Fig. 3-26).

Accelerometer PCB 352C33 (frequency interval of 0.5~10000Hz and sensitivity of 102 mV/g) (see Fig. 3-27).

Data acquisition system AD-Link (see Fig. 3-28).

Signal analysis software Visual Signal (see Fig. 3-5)

Resonant Frequency and Damping Analyzer (RFDA Basic) (see Fig. 3-11).

Chapter 4 Experimental results and discussions

Material properties

Compressive strength is one of the main characteristic of the concrete. For the impact test at early ages it is a key parameter to ensure that the beam concrete specimen will not be broken under the impact. At the age of 7 days it was found to be 36.56 MPa and reached 49.22 MPa at 28 days. Such a high compressive strength at early ages provides safe test conditions for the impact interaction test. Graphically, it is depicted in Fig. 4-. Average Dynamic Young's modulus and average Dynamic Shear modulus from 7 to 28 days are increased by 14.63% and 15.2%, respectively, and after that the changes become less significant. Graphically it is presented in Fig. and Fig. . Dependence of the dynamic Poisson's ratio on the ages of concrete is shown in Fig. . An average ultrasonic pulse velocity (see Fig.) varies from 4236 to 4581 m/s between 7 and 28 days. Such a behavior was expected, since the ultrasonic pulse velocity increases with increase of elastic properties of the material and its compressive strength as well. Therefore, there are no any internal cracks or defects of the concrete material detected.

Impact interaction test results

The main goal for the impact test was to define the contact duration as well as contact force during the impact of a steel rod upon a concrete beam specimen of Timoshenko type. The contact time dependencies on the age of concrete for the beam specimens #1, #2 and #3 are shown graphically in Fig. , Fig. and Fig. , respectively. Comparison of average values of contact duration vs. the age of concrete for three different concrete beam samples is shown in Fig. . It is obvious that the contact time decreased with concrete age. Average contact time between 7 and 14 days was reduced by 48.92% for beam specimen #1, by 48.08% for beam specimen #2 and for 47.63% for beam specimen #3. Between 14 and 28 days, so that the reduction of average contact time was 16.12%, 17.01% and 16.20%, accordingly. Between 28 and 56 days the decrease of the contact time was 11.34%, 11.18% and 11.35% for beam specimens #1, #2, and #3, respectively. Between 56 and 91 days, the decrease was 7.98%, 7.36% and 8.20% for beam specimens #1, #2, and #3, respectively. Finally, between 91 and 182 days the decrease values were 5.84%, 5.44% and 5.70%, correspondingly. It is obvious that after 28 days the changes of contact time became less significant.

Since contact force during the impact was not a constant, but a function of time (see Fig. 3-7), the maximum contact force was considered. Dependencies of the maximum contact force on concrete age for beam specimens #1, #2 and #3 are depicted in Fig. , Fig. ,
and Fig. , respectively. As it can be observed from the plots, the maximum contact force increases with concrete age. Comparing average values of maximum contact force for different beams (see Fig.), the one may conclude that the most remarkable change occurs before 14 days with the increase ratios of 29.29%, 29.60% and 32.36%, respectively, for beam specimens #1, #2 and #3. Between 14 and 28 days the increase ratios of such change become 10.02%, 9.20% and 7.90%, correspondingly. Between 28 and 56 days the values were 1.34%, 2.40% and 2.15%, accordingly. Between 56 and

91days the change rates were 2.82%, 1.40% and 1.88% for beam specimens #1, #2 and #3, respectively. Finally, between 91 and 182 days, contact force was increased by 1.17%, 1.37% and 1.84%, correspondingly, which is insignificant.

The trends of variations for both two parameters, the reduction of contact time and the increase of maximum contact force, could be explained by the progressive hardening process of the concrete specimens. When the concrete is fresh, it behaves like a viscos material. At this stage the contact time is the longest and the contact force is minimal due to relatively high value of concrete damping and, therefore, resulting in the high energy dissipation. After the concrete is gradually hardening, the internal friction is reducing and the energy dissipation is becoming less than the previous values during the impact. This leads to the increase of contact force and the decrease of contact duration. The decrease of internal friction with concrete age is discussed below.

When the maximum contact force is determined, the contact stress can be calculated accordingly. By dividing maximum contact force by contact area, the contact stress is calculated. For instance, by taking the highest value of the maximum contact force at all the ages of 40N and having the contact area of $20\ mm \times 20\ mm = 400\ mm^2$, the contact stress is given as follows,

$$\sigma_{cont} = \frac{40N}{400\ mm^2} = \frac{40N}{4 \cdot 10^4 m^2} = 10^5 Pa = 0.1MPa$$

It is obvious that the highest value of the contact stress exerted on the concrete beam specimens during the experiment was always much less than the ultimate strength of concrete at any ages. It means that the impact experiment of concrete beam specimen with the selected various impactors would not result in any structural damage to the concrete beam specimens at any ages.

Internal friction test results

The results of damping test are shown in Fig. . According to the data, the most significant changes (in absolute values) for all the concrete specimens occur at the early ages before 14 days. However, by taking into account relative values of the damping changes, it should be noted that this process of progressive changes of concrete properties has been continuously going through all the periods of concrete ages. This phenomenon could be explained by dislocation damping in molecular structure of the material, which was referred as the Granato-Lucke Theory [12], in which the string model could describe damping in materials from the microstructural point of view. According to the model, material properties can be modeled by an elastic string vibrating in a viscous medium. During concrete setting and hardening, the viscosity is reduced substantially, which, in turn, causes the decrease of internal friction in concrete. Moreover, from the macro-structural point of view, during its setting and hardening, concrete possesses a phase transformation from liquid to solid, from viscous to elastic stage. Phase lag between stress and strain, or, mechanical loss is defined in literature as internal friction [13], [14]. Reduction of internal friction with age can also be explained by the fact that when the material becomes more elastic, applied strain will have less phase lag with the stress in the material. Therefore, internal friction value for the same concrete material will be reducing with concrete hardening and, therefore, with its aging.

Vector diagrams and fractional parameter

The dependencies of the real and imaginary parts of complex modulus on frequency were constructed and are shown for beam specimens 1, 2, and 3 in Fig. - Fig. , respectively. Considering dependency of Elastic Loss Modulus on frequency, a peak on the graph can be observed. This phenomenon is commonly mentioned in the literature [15] and is related to intensive phase transformation in the material at this age [16].

By eliminating the frequencies from these graphs, the vector diagrams were constructed for three different beam specimens (see Fig. - Fig.). These diagrams are very important to describe the behavior of the fractional parameter γ of concrete material. By using these diagrams, the values of γ serving as the main factor to control viscosity of the concrete material can be measured as the slope of the curve at the beginning and at the end in the diagram. A typical regression equation of the curve in the diagram as shown in fig. 5-21 can be found as

$$y(x) = \ 0.00205x^3 - \ 0.24315x^2 + \ 9.46410x - 120.92887 \ ,$$

and its first derivative $\frac{dy(CS1)}{dx} = 0.00615x^2 - 0.48631x + 9.46410$

By taking into account the geometrical meaning of first-order derivative, the fractional parameter γ can be calculated for each end of the diagram.

$$\gamma_7^{CS1} = \left.\frac{dy}{dx}\right|_{x=31.22916} = 0.27490,$$

$$\gamma_{182}^{CS1} = \left|\left(\left.\frac{dy}{dx}\right|_{x=39.61401}\right)\right| = |-0.14958| = 0.14958.$$

Roots $x_1 = 31.22916,\ x_2 = 39.61401$ of the equation

$$0.00205x^3 - \ 0.24315x^2 + \ 9.46410x - 120.92887 \ = 0,$$

are obtained numerically (the third root $x_3 = 47.62644$) is excluded since it falls out of the interval of our interest. The second parameter is taken with its absolute value due to the properties of *tan(x)*. Since *tan(180°-x)=-tan(x)*, where x<90°, the negative slopes are obtained for tan(180°-x), after transformation to tan(x) become positive.

When fractional parameters at the end points of the vector diagram are known, they can be represented as a curve showing its dependence on age (see Fig.). The fractional parameters for beam specimen #2 and beam specimen #3 were obtained by the same way. As it can be seen for the plot, an average fractional parameter between the ages of 7 and 182 days was decreased by 107.12%, which is more than two times to the original value. This trend is closely related to changes of concrete properties during its progressive hardening process. The viscos properties of concrete beam specimens are gradually going down, whereas the elastic properties of concrete beam specimens are steadily more and more dominating.

Chapter 5 Conclusions and recommendations

Conclusions

Based on the results of this study the following conclusions have been made.

I. Two methods are combined to find the solution of the stated problem:
   1. The ray method, which is applied for constructing an approximate solution within outside of the contact zone and the exact solution within the disturbed domain of the elastic rod.
   2. Laplace transformation method for determination of the contact force within the contact domain. It could be utilized to solve the linear equation for the contact force, since the Hertz contact theory is inapplicable for the case of the impactor with a flat end.

   Having a good agreement with the experimental results, these two methods complete each other and provide solutions for the beam in both, outside and inside the contact area as well as for the rod.

II. One-term ray expansions are suggested to be applied in such problems to find the contact force and longitudinal and transverse forces applied to the boundary of the contact region. They are used in the problem under consideration, since the contact duration is a small value. This fact provides the convergence of the ray expansions, since the argument of the expansion is a small value.

III. From the experimental part of current study, it was found that:
   1. Contact time decreases with concrete age: average value between 7 and 182 days was decreased from 442 μs to 202 μs with rate of 54.29%.
   2. Maximum contact force increases with concrete age: average value between 7 and 182 days was increased from 24.16 N to 39.81 N with rate of 39.31%.
   3. Internal friction was decreased with concrete age: average value between 7 and 182 days has been decreased from 0.019424 to 0.003948 with rate of 97.96%. The most significant changes (in absolute values) occur before 14 days. It is found to be a very important characteristic governing the changes of concrete behavior with its aging.
   4. Fractional parameter decreases with concrete age: average value between 7 and 182 days has been decreased from 0.279 to 0.135 with rate of 51.62%. It is an additional structural parameter for concrete, which is able to describe the material properties changes under the impact taking into account aging of concrete.

IV. Since structural concrete elements sometimes are subjected to the impacts during construction and their service life, the method proposed in this study could be applied to evaluate safety of using the concrete beam after the impact. As a first step to evaluate the damage of the real concrete beam is the identification of internal friction in undamaged material with corresponding material constants and fractional parameter obtained from the vector diagrams. This step must be done for damaged area as well. After the material constants in damage area are known, contact force can be calculated according to proposed analytical model. When the

contact force is known, the contact stress can be calculated and after the comparison with ultimate stress, safety condition can be verified. In case of damage, the degree of damage can be estimated by comparison of the internal friction and fractional parameter of undamaged and damaged materials. After that the final estimation of the severity of the impact can be done.

Recommendations

There are some recommendations can be given for the application of the method.

1. In order to construct the vector diagrams and measure fractional parameter, any suitable method of internal friction measurement can be applied.
2. In order to identify the severity of the structural damage, as an additional verification method, it is also recommended to use modern scientific equipment, such as x-ray machines, etc.
3. The problem could be extended for the case of round-ended impactor, which will allow to use Hertz's contact theory to describe non-linear cases, however it requires additional theoretical investigations.

Acknowledgements

We would like to express our deepest appreciation to Ministry of Science and Technology of Taiwan (former Taiwan National Science Council) and the Russian Foundation for Basic Research for the financial support of this project. We also appreciate to National Taiwan University of Science and Technology for providing a perfectly-equipped laboratory for the experimental work, to Research Center on Dynamics of Solids and Structures at Voronezh State University of Architecture and Civil Engineering, Prof. Shitikova Marian V. and Prof. Rossikhin Yurii A. for the valuable theoretical input in the project.

References

1. "Global Construction Outlook 2020," Timetric, 2015.
2. Rossikhin Yu.A., Shitikova M.V., “The analysis of the impact response of a thin plate via fractional derivative standard linear solid model, Journal of Sound and Vibration, Vol.330, pp. 1985-2003, 2011.
3. Rabotnov, Y., "Equilibrium of an elastic medium with after-effect (English translation)," Fractional Calculus and Applied Analysis, vol. 17, no. 3, pp. 684-696, September 2014.
4. Rossikhin, Y. A. and Shitikova, M. V., "Application of Fractional Calculus for Dynamic Problems of Solid Mechanics: Novel Trends and Recent Results," Applied Mechanics Reviews, vol. 63, no. 1, pp. 01801-1 - 01801-52, January 2010.
5. Rossikhin, Y. A.and Shitikova, M. V., "The ray method for solving boundary problems of wave dynamics for bodies having curvilinear anisotropy," Acta Mechanica, vol. 109, no. 1, pp. 49-64, March 1995.
6. Rossikhin, Y. A. and Shitikova, M. V., "Transient response of thin bodies subjected to impact: wave approach," Shock and Vibration Digest, vol. 39, no. 4, pp. 273-309, July 2007.
7. Rossikhin Yu.A., Shitikova M.V. //Proceedings of the IFIP W67.2 on Modelling and Optimization of Distributed Parameter Systems with Application to Engineering, Warsaw, Poland, June 1995, Chapman & Hall, pp. 370-374
8. ASTM C494 / C494M - 15a, Standard Specification for Chemical Admixtures for Concrete, West Conshohocken, PA: ASTM International, 2015.
9. ASTM C39 / C39M - 15a, Standard Test Method for Compressive Strength of Cylindrical Concrete Specimens, West Conshohocken, PA: ASTM International, 2015.
10. ASTM E1876-09, Standard Test Method for Dynamic Young's Modulus, Shear Modulus, and Poisson's Ratio by Impulse Excitation of Vibration, West Conshohocken, PA: ASTM International, 2009.
11. ASTM C597 - 09, Standard Test Method for Pulse Velocity Through Concrete, West Conshohocken, PA: ASTM International, 2009.
12. Meshkov, S., Viscoelastic properties of metals (In Russian), Moscow: Metallurgia, 1974, p. 193.
13. Blanter, M., Golovin, I., Neuhausser, H.and Sinning, H.-R., Internal Friction in Metallic Materials, vol. 90, R. Hull, J. Parisi, R. M. Osgood and H. Warlimont, Eds., Springer Berlin Heidelberg, 2007, p. 539.
14. Postnikov, V., Internal friction in metals (In Russian), Moscow: "Metallurgy", 1974.

15. Oeser, M. and Pellinien, T., "Computational framework for common visco-elastic models in engineering based on the theory of rheology," Computers and Geotechnics, vol. 42, pp. 145-156, 2012.
16. Fowler, B. L., Interactive characterization and database storage of complex modulus data, Palo Alto, California, 1989.

Table of Tables

Table 3-1 Chemical composition and physical properties of ordinary Portland cement OPC)

Composition/Properties of OPC	
Chemical compositions,	%
SiO_2	20.42
Al_2O_3	4.95
Fe_2O_3	3.09
CaO	61.96
MgO	3.29
SO_3	2.4
LOI	1.75
Physical properties	
Specific gravity (g/cm^3)	3.15
Specific surface (cm^2/g)	3450
Initial setting time (h)	2.58
Final setting time (h)	4.34

Table 3-2 Physical properties of aggregates

Properties	Coarse Aggregate	Fine Aggregate
D_{max}, mm	15.0	-
Specific gravity (OD)	2.70	2.63
Fineness modulus	6.58	2.73
Water absorption, %	0.56	1.78

Table 3-3 Mix proportions per 1 m^3 of concrete according to ACI 211.1 method

Components	Water	Cement	Fine agg.	Coarse agg.	Superplasticizer
kg/m^3	194.00	554.29	708.33	932.38	2.20

Table 3-4 Damping test results of reference sample: reference impactor

Flextural mode			Torsional mode			E, GPa	G, GPa	Poisson ratio
Frequency, Hz	Loss rate	Damping	Frequency, Hz	Loss rate	Damping			
8168.61	31.1	0.001211	*10488.4*	29	0.00088	**209.42**	**80.55**	0.3
8168.27	29.8	0.001159	*10488.5*	28	0.000849	**209.4**	**80.55**	0.3
8168.91	27.2	0.001058	*10487.2*	29.5	0.000895	**209.44**	**80.53**	0.3
8168.72	25.1	0.000977	*10489.6*	23.8	0.000721	**209.42**	**80.57**	0.3
8168.55	25.9	0.001009	*10488.5*	25.9	0.000787	**209.41**	**80.55**	0.3
8168.79	24.9	0.000969	*10488.6*	24.3	0.000736	**209.43**	**80.55**	0.3
8168.56	23.6	0.000919	*10488.5*	22.4	0.000681	**209.41**	**80.55**	0.3
8168.9	25.3	0.000985	*10489.2*	23.8	0.000723	**209.43**	**80.56**	0.3
8168.37	23.9	0.000931	*10488.5*	29.2	0.000886	**209.4**	**80.55**	0.3
8168.57	24.9	0.000969	*10489.4*	36.3	0.001103	**209.41**	**80.56**	0.3
8168.39	23.1	0.000899	*10488.7*	22.3	0.000676	**209.4**	**80.55**	0.3

Table 3-5 Damping test results of reference sample: spherical impactor of 15.88 mm in diameter

Flextural mode			Torsional mode			E, GPa	G, GPa	Poisson ratio
Frequency, Hz	Loss rate	Damping	Frequency, Hz	Loss rate	Damping			
8168.43	23.6	0.000918	*10489.2*	24.9	0.000757	**209.41**	**80.56**	0.3
8168.75	21.4	0.000832	*10488.7*	33.1	0.001005	**209.42**	**80.55**	0.3
8170.03	27.2	0.00106	*10488.6*	26.4	0.0008	**209.49**	**80.55**	0.3
8169.07	21.3	0.000832	*10487.7*	28.9	0.000878	**209.44**	**80.54**	0.3
8169.51	20.6	0.000803	*10487.9*	22.2	0.000674	**209.47**	**80.54**	0.3
8169.53	22.9	0.000893	*10489.6*	26.1	0.000792	**209.46**	**80.57**	0.3
8169.77	25.6	0.000999	*10489.4*	28.6	0.000867	**209.48**	**80.56**	0.3
8170.38	24.3	0.000945	*10491.1*	24.9	0.000755	**209.51**	**80.59**	0.3
8170.89	22.6	0.000881	*10490.5*	29.7	0.000901	**209.54**	**80.58**	0.3
8170.14	24.7	0.000963	*10490.7*	26.6	0.000808	**209.5**	**80.58**	0.3

Table 3-6 Damping test results of reference sample: spherical impactor of 9.50 mm in diameter

Flextural mode			Torsional mode			E, GPa	G, GPa	Poisson ratio
Frequency, Hz	Loss rate	Damping	Frequency, Hz	Loss rate	Damping			
8170.79	25.8	0.001007	*10489.4*	24.9	0.000755	**209.53**	**80.56**	0.3
8170.87	24.6	0.00096	*10491.3*	24.4	0.000739	**209.53**	**80.59**	0.3
8171.03	25.9	0.001009	*10492.3*	28.6	0.000868	**209.54**	**80.61**	0.3
8171.17	24.5	0.000953	*10491.2*	25.8	0.000784	**209.55**	**80.59**	0.3
8171.12	24.5	0.000956	*10491.1*	27.9	0.000848	**209.55**	**80.59**	0.3
8171.16	24.3	0.000945	*10491.4*	25.5	0.000774	**209.55**	**80.59**	0.3
8171.07	22.8	0.00089	*10493*	27.2	0.000824	**209.54**	**80.62**	0.3
8171.24	23.2	0.000905	*10491.5*	25.6	0.000776	**209.55**	**80.6**	0.3
8171.17	25	0.000976	*10491.5*	25.5	0.000773	**209.55**	**80.6**	0.3
8171.58	25.1	0.000976	*10491.4*	22.8	0.000693	**209.57**	**80.59**	0.3

Table 3-7 Damping test results of reference sample: spherical impactor of 7.14 mm in diameter

Flextural mode			Torsional mode			E, GPa	G, GPa	Poisson ratio
Frequency, Hz	Loss rate	Damping	Frequency, Hz	Loss rate	Damping			
8172.15	23.5	0.000916	*10492.8*	39.3	0.001192	**209.6**	**80.62**	0.3
8171.92	21.5	0.000839	*10492.2*	21.3	0.000645	**209.59**	**80.61**	0.3
8172.3	24.6	0.00096	*10491.6*	22.6	0.000685	**209.61**	**80.6**	0.3
8171.56	24.1	0.000937	*10491*	31.9	0.000969	**209.57**	**80.59**	0.3
8171.53	25.1	0.000979	*10491.4*	33.2	0.001007	**209.57**	**80.59**	0.3
8171.91	23.6	0.000918	*10492.1*	30.5	0.000924	**209.59**	**80.6**	0.3
8171.89	23	0.000897	*10493*	26.9	0.000815	**209.58**	**80.62**	0.3
8171.75	21.6	0.000839	*10490.5*	34.7	0.001053	**209.58**	**80.58**	0.3
8171.8	22.6	0.000878	*10492.2*	25.1	0.000761	**209.58**	**80.61**	0.3
8171.89	25.7	0.001001	*10492.7*	25.7	0.00078	**209.59**	**80.61**	0.3

Table of Figures

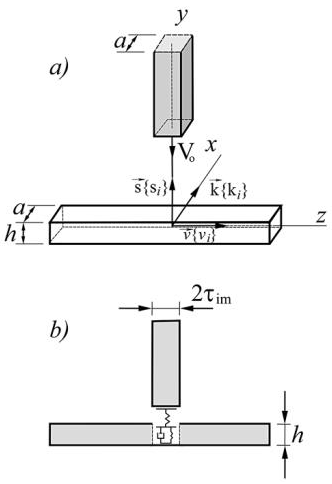

Fig. 2-1 Problem formulation

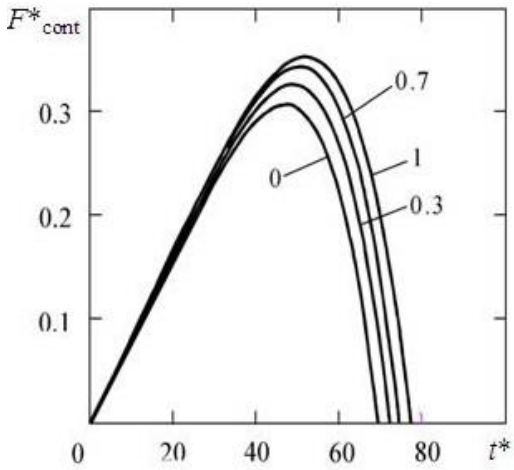

Fig. 2-2 Dimensionless contact force vs. dimensionless time.

Fig. 3-1 Slump test of fresh concrete

Fig. 3-2 Concrete beam specimens

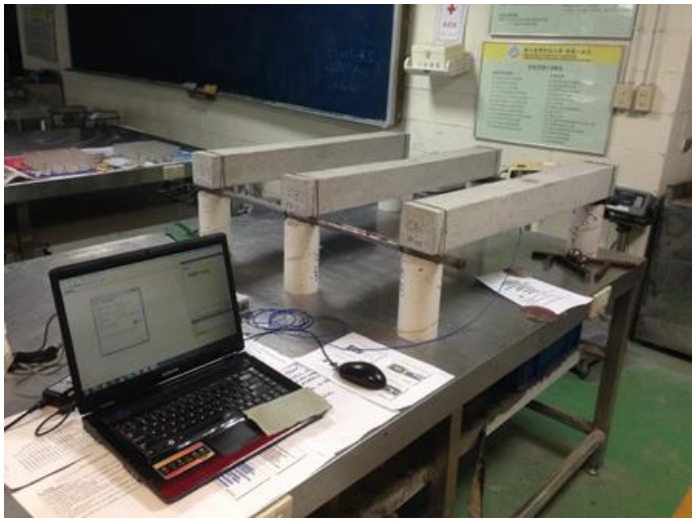

Fig. 3-3 Experimental setup for the impact test

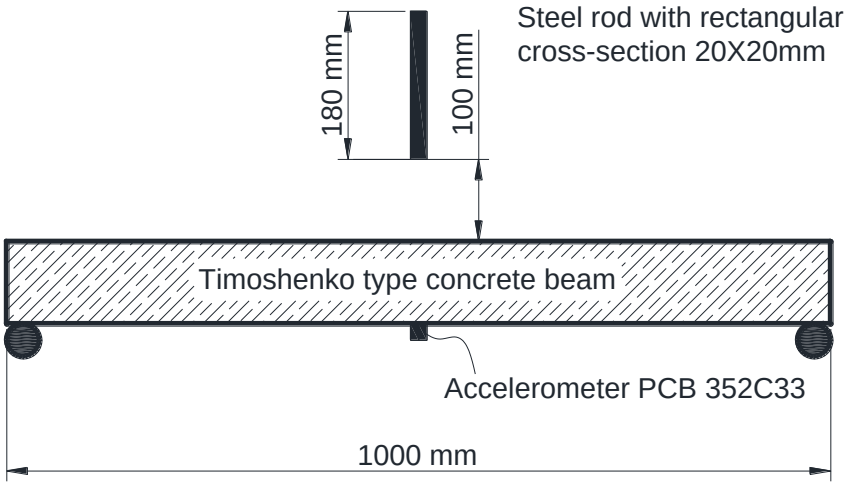

Fig. 3-4 Schematic diagram for the impact test

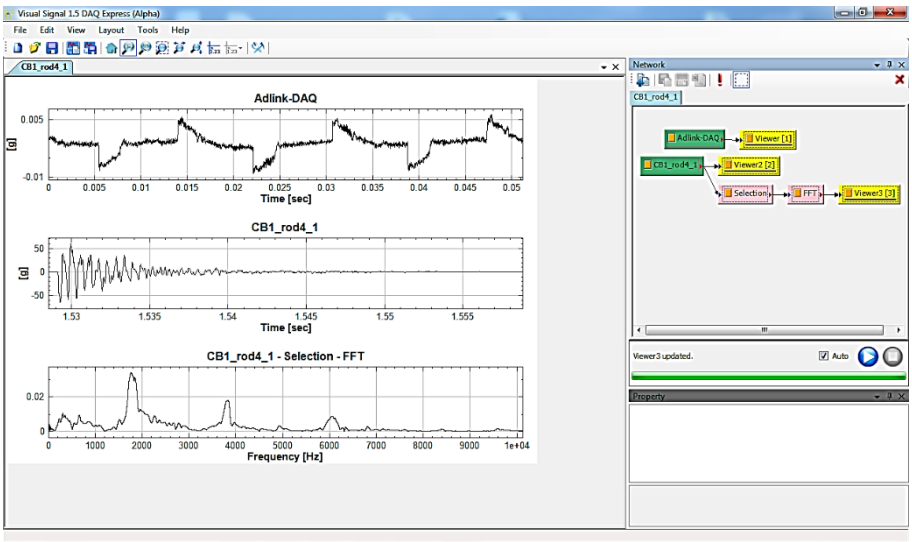

Fig. 3-5 Visual Signal software interface

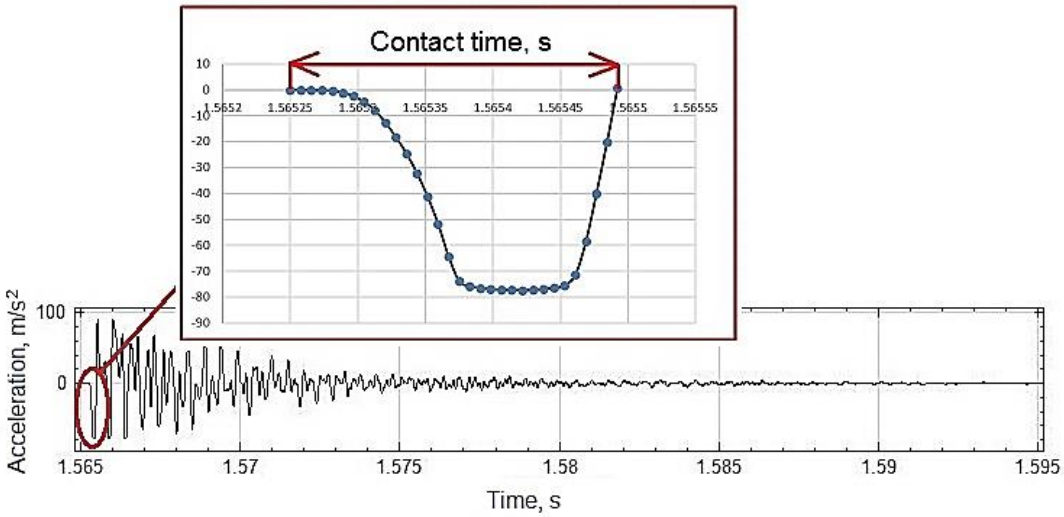

Fig. 3-6 Contact time measurement

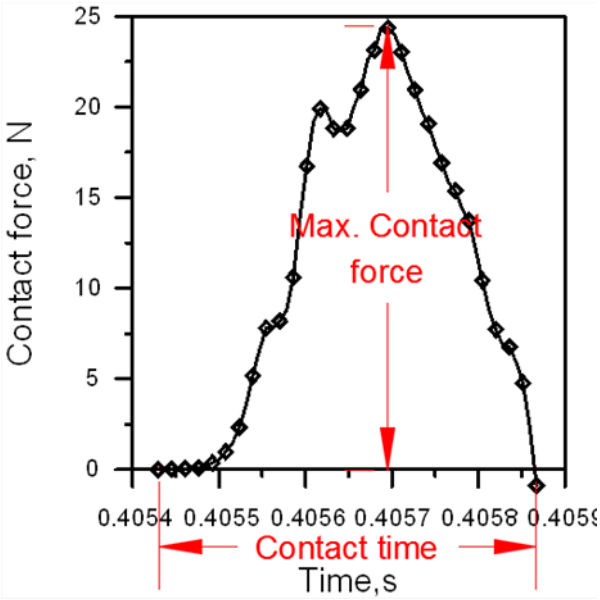

Fig. 3-7 Graphical identification of the contact force during the impact process

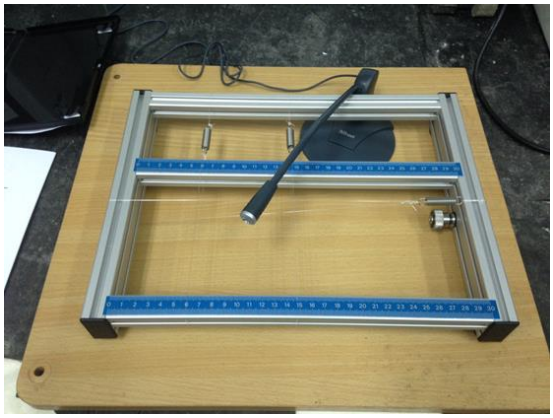

Fig. 3-8 Original universal wire support for RFDA Basic

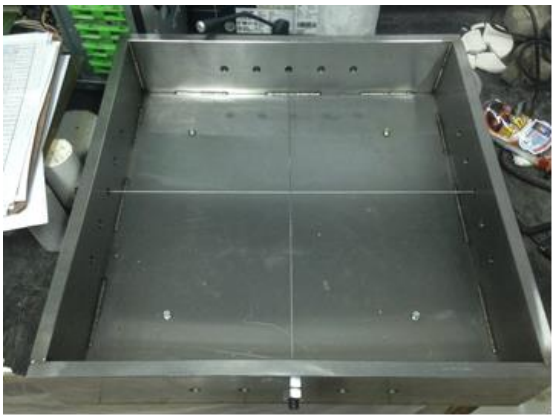

Fig. 3-9 Steel wire support designed by the author

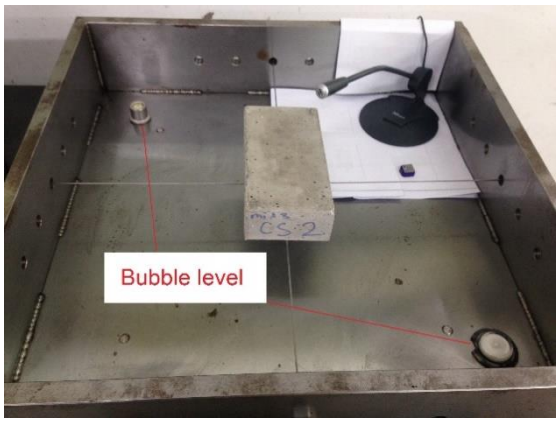

Fig. 3-10 Bubble level instruments for of the horizontalness verification of the support

Fig. 3-11 Internal friction experimental setup

Fig. 3-12 Digital caliper “Metrology” (Photo of the original device)

Fig. 3-13 Inspection certificate for the digital caliper “Metrology”(Photocopy of the original inspection certificate provided by the manufacturer)

Fig. 3-14 Electronic weigher JADEVER 3016

Fig. 3-15 Electronic weigher Shimadzu TX4202L

Fig. 3-16 Oven for curing aggregates and samples

Fig. 3-17 Grinding Machine

Fig. 3-18 Big concrete mixer

Fig. 3-19 Medium concrete mixer

Fig. 3-20 Small concrete mixer

Fig. 3-21 Horizontal table for the smoothness verification of sample ends

Fig. 3-22 Computer-Control Servo Hydraulic Concrete Compression Testing Machine HT-8391PC

Fig. 3-23 Dynamic Resonant Frequency Instrument “ERUDITE”

Fig. 3-24 Ultrasonic Pulse Velocity Meter “Pundit 7”

Fig. 3-25 Vibrating table

Fig. 3-26 Bubble level instruments

Fig. 3-27 Accelerometer

Fig. 3-28 Data acquisition system AD-Link

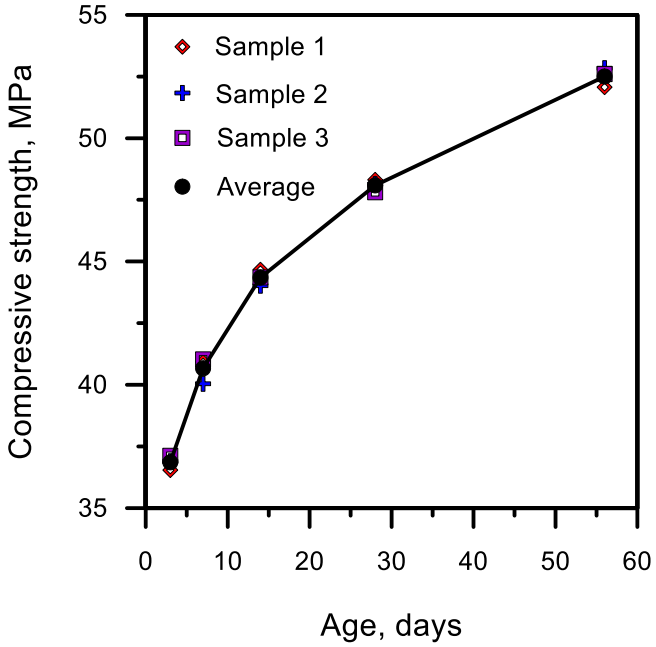

Fig. 4-1 Compressive strength development

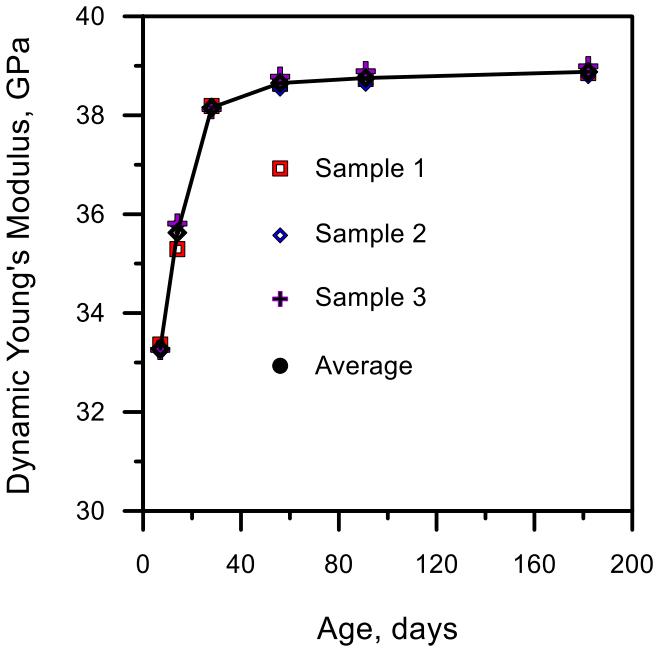

Fig. 4-2 Dynamic Young's Modulus vs. age

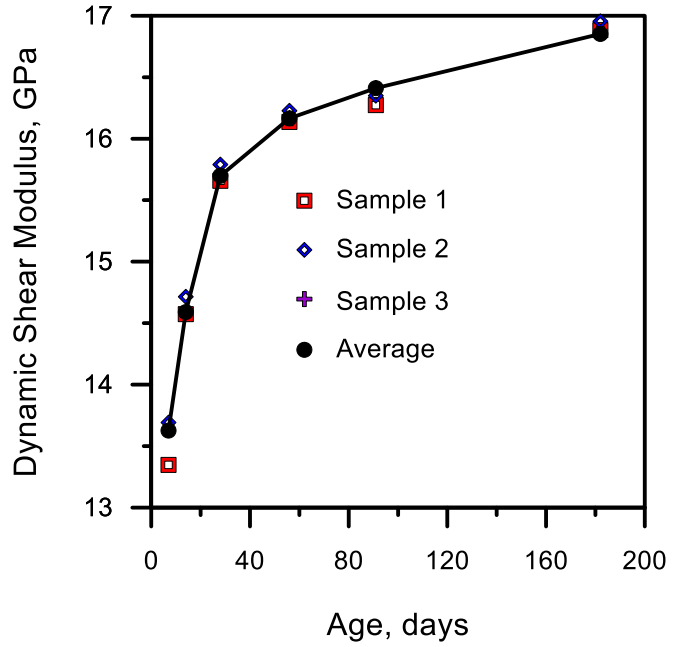

Fig. 4-3 Dynamic Shear Modulus vs. age

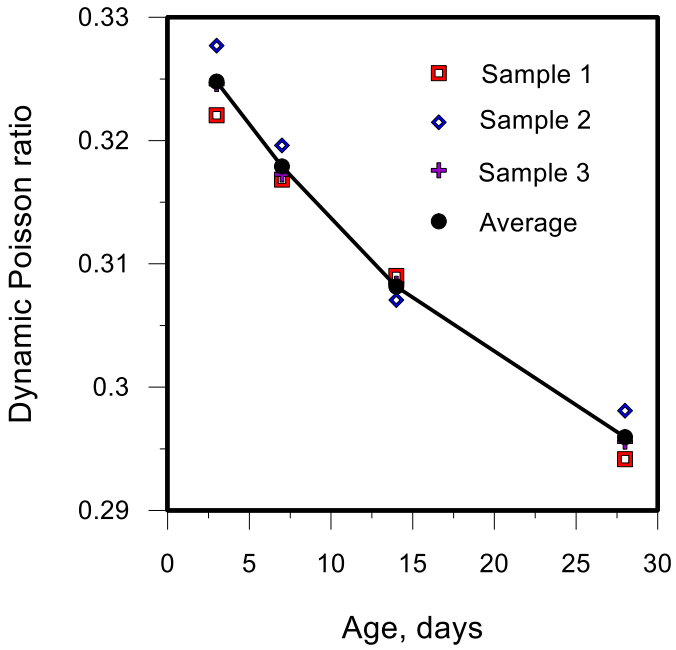

Fig. 4-4 Dynamic Poisson's Ratio vs. time

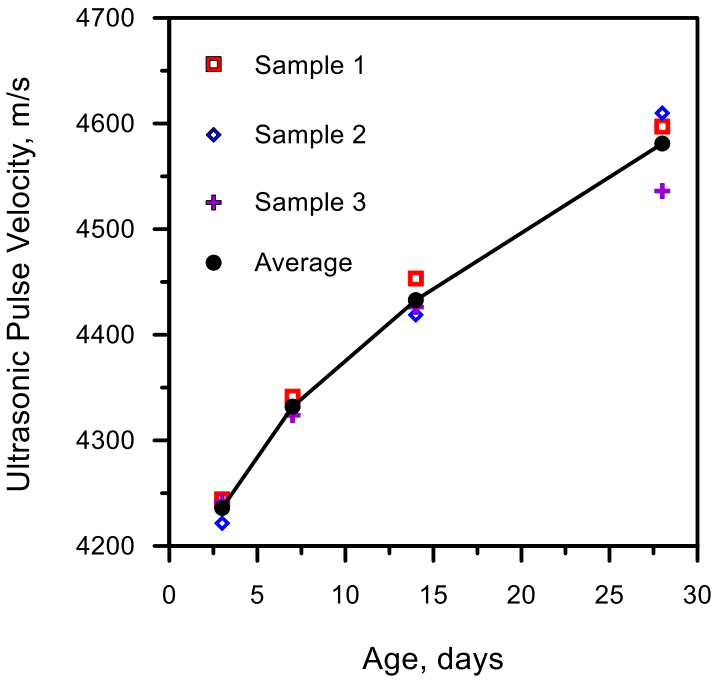

Fig. 4-5 Ultrasonic pulse velocity vs. time

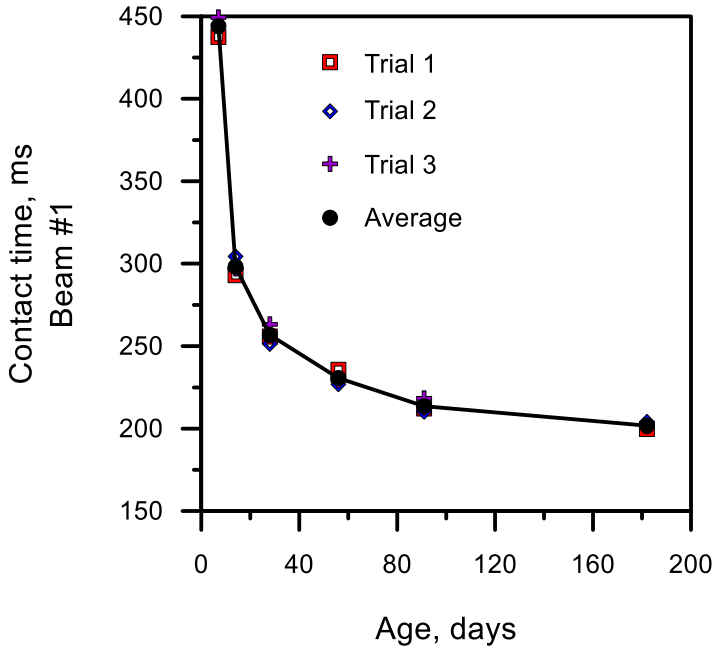

Fig. 4-6 Contact time vs. age, Beam #1

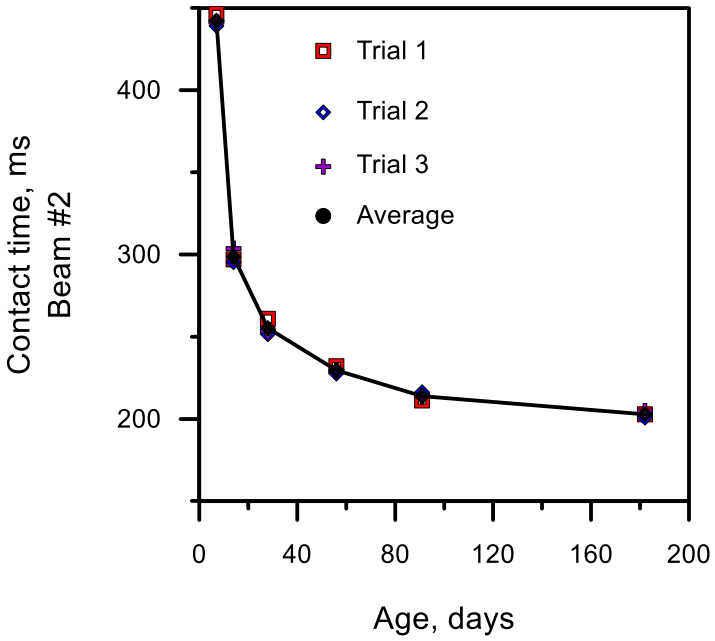

Fig. 4-7 Contact time vs. age, Beam #2

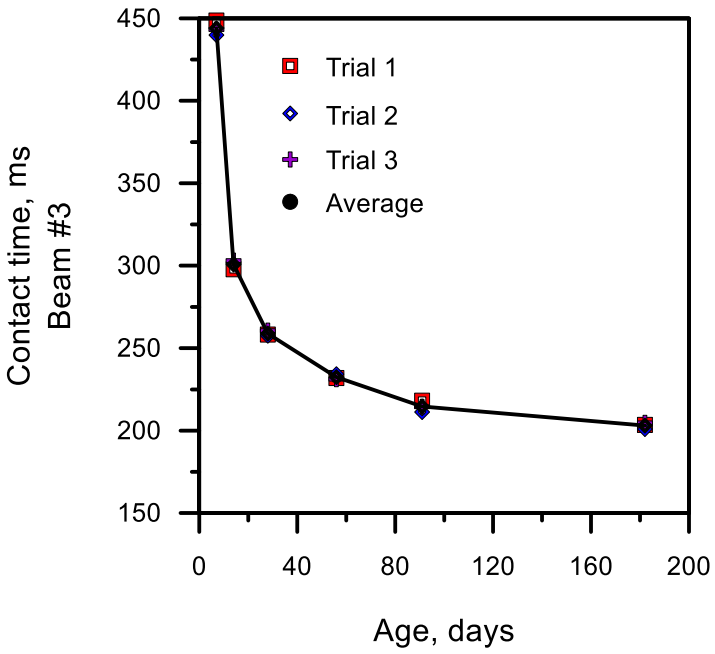

Fig. 4-8 Contact time vs. age, Beam #3

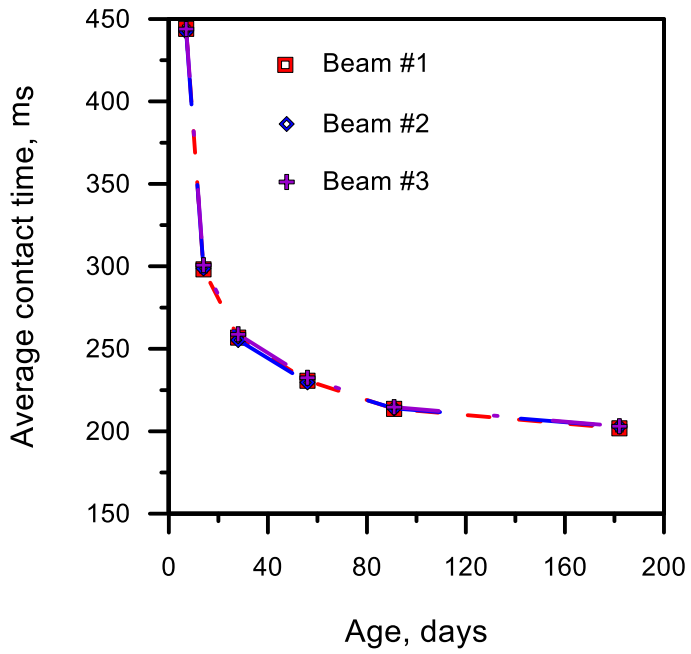

Fig. 4-9 Comparison of average contact times measured on different beams

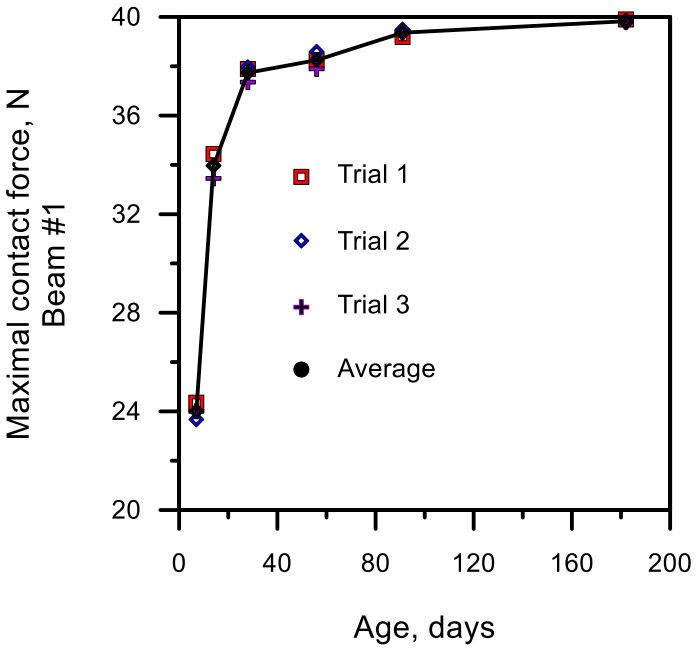

Fig. 4-10 Maximal contact force vs. age, Beam #1

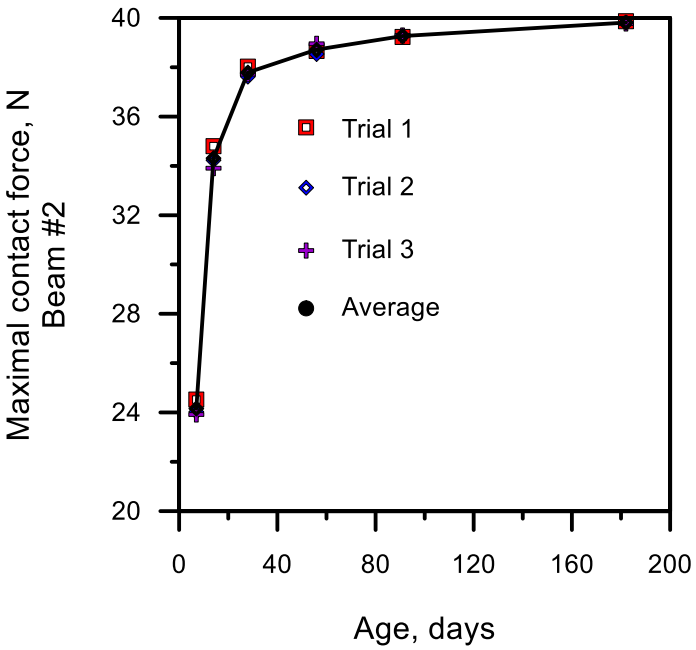

Fig. 4-11 Maximal contact force vs. age, Beam #2

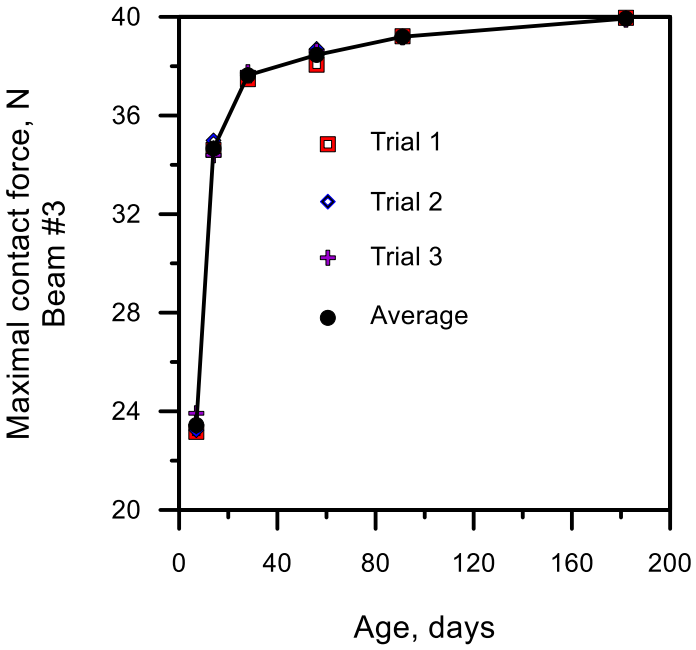

Fig. 4-12 Maximal contact force vs. age, Beam #3

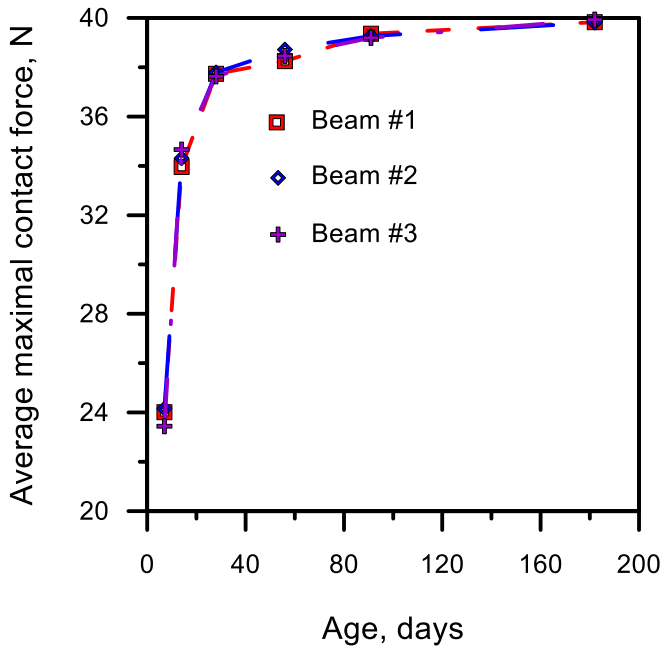

Fig. 4-13 Comparison of average maximal contact forces measured on different beams

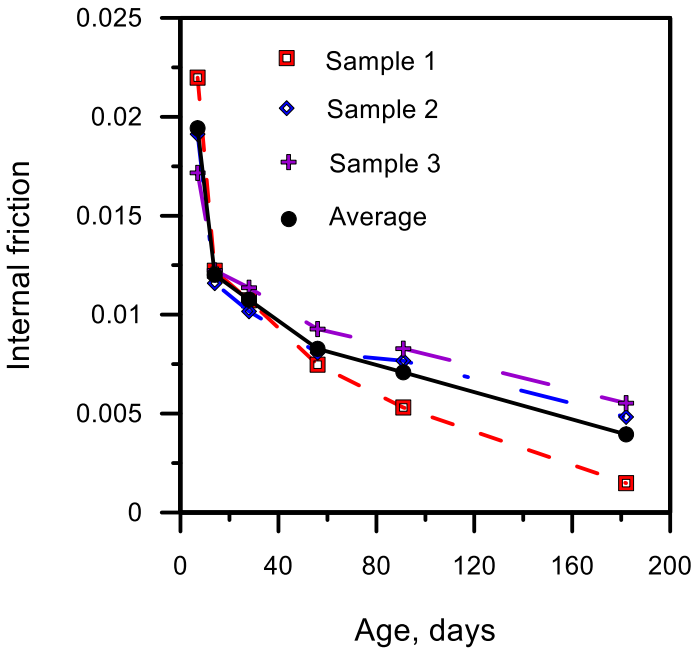

Fig. 4-14 Internal friction vs. age

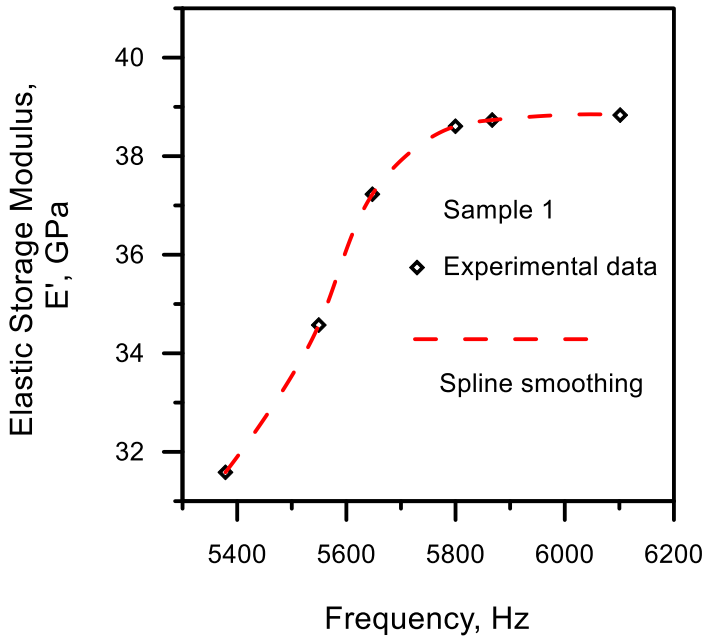

Fig. 4-15 Elastic Storage Modulus vs. frequency, specimen #1

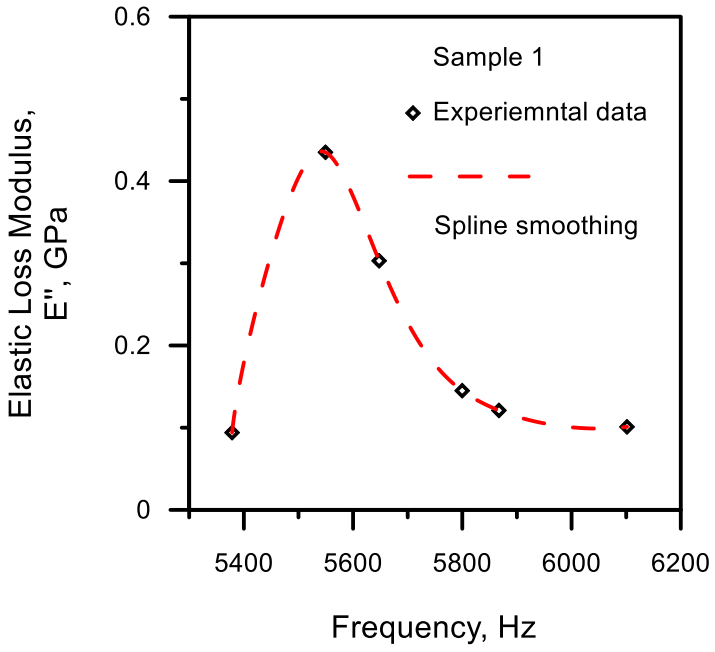

Fig. 4-16 Elastic Loss Modulus vs. frequency, specimen #1

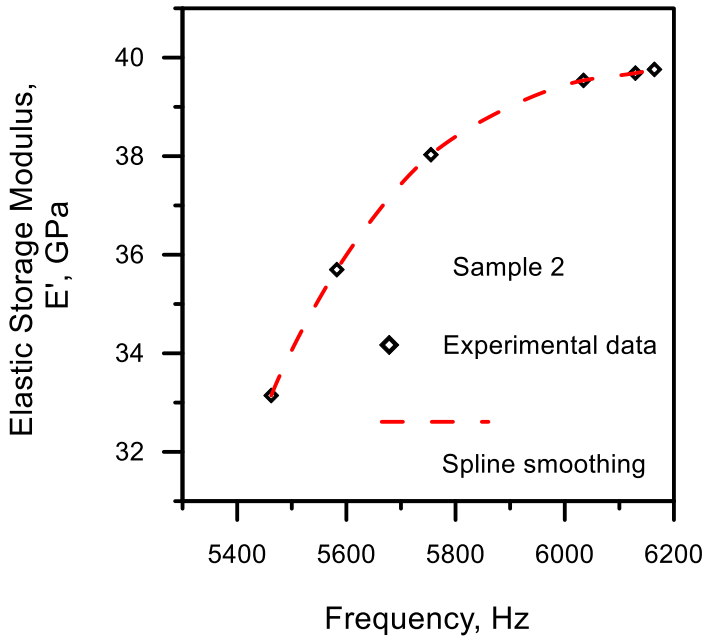

Fig. 4-17 Elastic Storage Modulus vs. Frequency, specimen #2

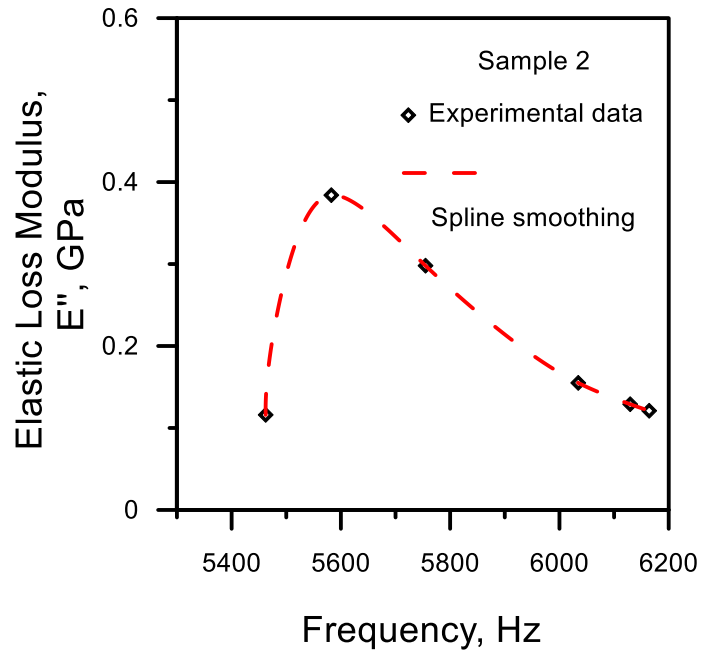

Fig. 4-18 Elastic Loss Modulus vs. frequency, specimen #2

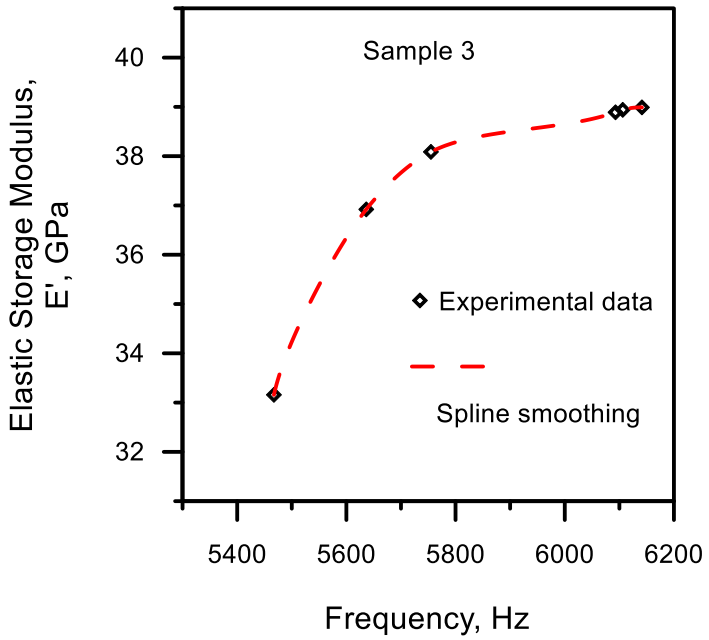

Fig. 4-19 Elastic Storage Modulus vs. frequency, specimen #3

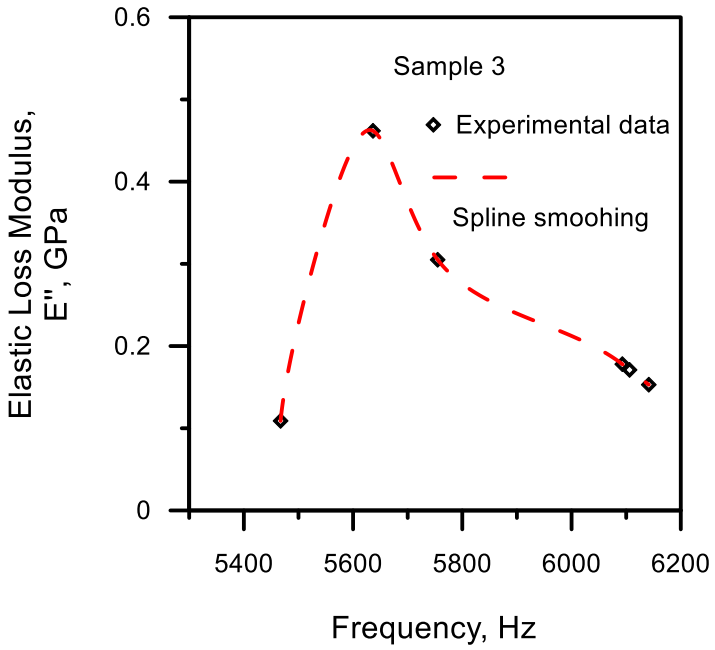

Fig. 4-20 Elastic Loss Modulus vs. frequency, specimen #3

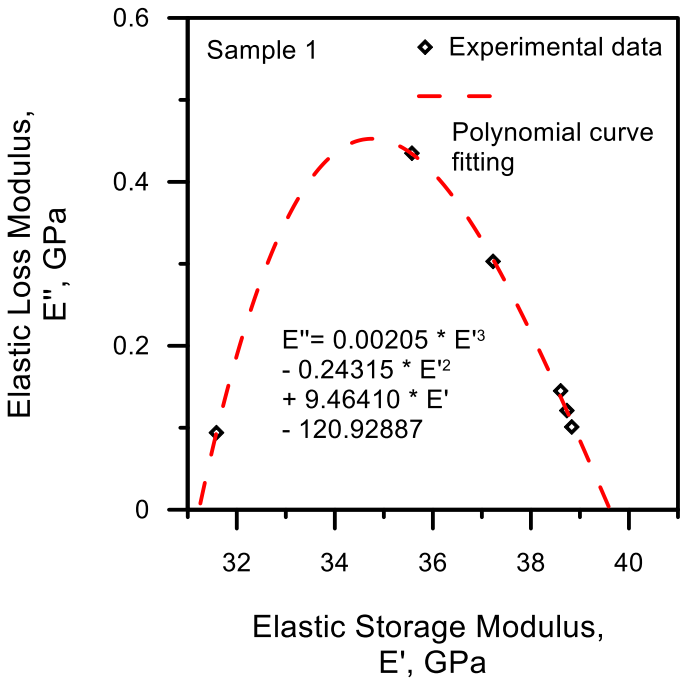

Fig. 4-21Vector diagram, specimen #1

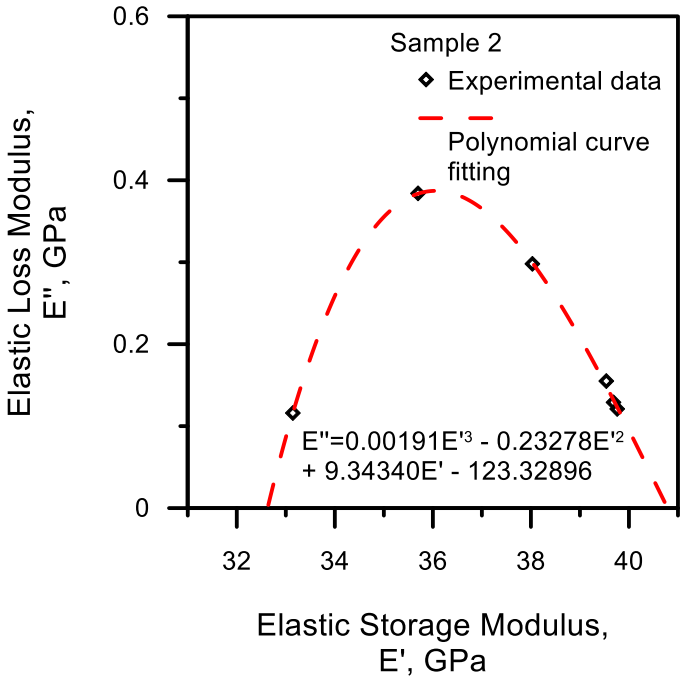

Fig. 4-22 Vector diagram, specimen #2

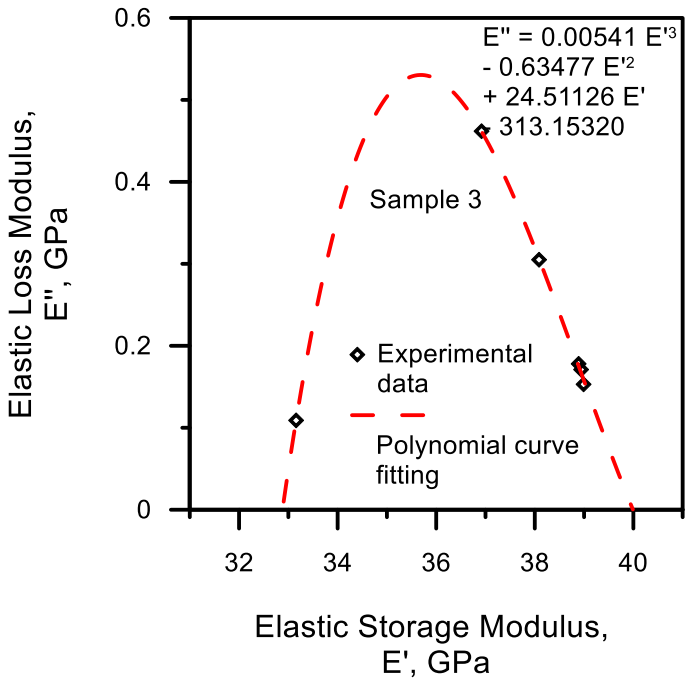

Fig. 4-23 Vector diagram, specimen #3

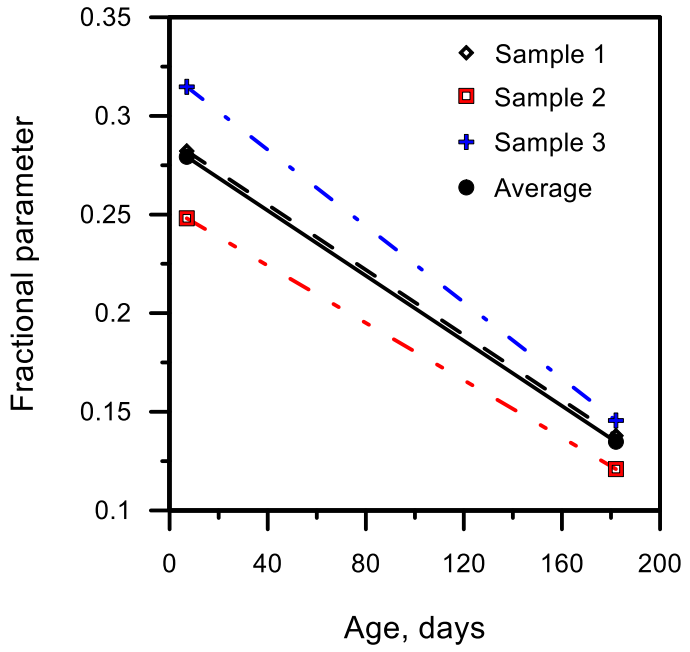

Fig. 4-24 Fractional parameter vs. age

Appendix 3

Statistic Data of the Join Research Cooperation

I. Number of Staff working in the joint project – the "staff type" including: principal investigator (PI), collaborating principal investigator (co-PI), assistant investigator, and postdoctoral research fellow.

Staff Type	Taiwan Side	Russia Side
PI and Co-PI	Distinguished Prof. Chang Ta-Peng	Full Prof. Shitikova Marina V., Distinguished Prof. Rossikhin Yurii A.
Full-time research assistant	Ph.D. candidate Popov Ivan	
Part-time research assistant	PH.D. student Hoang Anh Nguyen	Assistant prof. Nataliya A. Nekrasova, Ph.D. student Maria Estrada Mendos
Postdoctoral Research Fellow	Assistant Prof. Chen Chun-Tao	

II. Joint publication(s) (by the date of this report submitted)

1. Scientific Journal Information for Papers Being Published or Accepted

Title of Paper	Name of Journal	SCI/EI /SSCI	Impact Factor	Volume No.	Date
Impact response of a viscoelastic beam considering the changes of its microstructure in the contact domain	Mechanics of Time-Dependent Materials	SCI	1.587	Online	2015.08.04

2. Monographs and Articles in Books Being Published or Accepted

Title of Article, Monograph	Name of Book, Publishing House	SCI/EI/SSCI	Impact Factor

3. International or Domestic Conferences and Symposiums

Title of Paper	Name of Event	Organizer of the Event	Date
Centennial jubilee of Academician Rabotnov and contemporary handling of his fractional operator	International conference dedicated to centennial jubilee of Academician Rabotnov	Institute of Machines Science named after A. A. Blagonravov of the Russian Academy of Sciences	2014/02/24-2014/02/26
	ICAE 2014	International Journal of Applied Energy & National Taiwan University of Science and Technology	2014/05/30-2104/06/02
Dynamic response of a hereditarily elastic beam with Rabotnov's kernel impacted by an elastic rod	2014 International Conference on Mathematical Models and Methods in Applied Sciences (MMMAS '14)	Saint Petersburg, State Politechnical University	2014/09/23–014/09/25
Impact response of a viscoelastic beam considering the changes of its microstructure in the contact domain	The XIth All-Russian Congress on Basic Problems of Theoretical and Applied Mechanics	The Russian National Committee on Theoretical and Applied Mechanics jointly with the Kazan Federal University and the Institute of Mechanics and Mechanical Engineering of the RAS Kazan Scientific Center	20.08.2015 – 24.08.2015

Application of impulse excitation technique to investigation of concrete damping and its changes at early ages	2016 International Conference on Measurement and Test Methodologies, Technologies and Applications (MTMTA2016)	Phuket, Thailand	24.04.2016 – 25.04.2016
Study of concrete aging effect on the contact force and the contact time during the impact of an elastic sphere upon a viscoelastic beam	2016 International Conference on Measurement, Test and Industrial Application (ICMTIA 2016)	Chiang Mai, Thailand	26.06.2016 – 27.06.2016

4. Other Publishing Plan of Papers, Articles or Monographs [Submitting or Under-reviewing】

Title of Paper, Article or Monograph	**Name of Journal, Publishing House**	**SCI/EI/SSCI**	**Impact Factor**
Experimental study of concrete aging effect on the contact force and contact time during the impact interaction of an elastic rod with a viscoelastic beam	Journal of Mechanics	SCI	0.828

Appendix 3

III. Joint application for Patent rights or Technology transfer (if applicable)

□ **Patent** □ **Technology transfer**

Name of Invention or Technology	
Technology Description (max. 200 words)	
Technique Features	
Applicable Industry or Potential Product for Commercialization	
Patent Issued Country	
Patent Period	

Note: please don't describe the major content if you haven't got the patent issued

IV. Data of Personnel Exchange

1. Visiting Russia from Research Teams working in Taiwan

Date of Visiting	Main Task and Result	Total member of visiting team/country
2014/02/12 – 2014/03/22	Russian literature collecting, attending an International conference in Moscow, dedicated to centennial jubilee of Academician Rabotnov.	Ivan Popov
2014/06/15 – 2014/09/15	Theoretical studies, preparation for the paper publications, literature collection and writing experimental literature overview.	Ivan Popov
2014/09/11 – 2014/09/15	Visit Voronezh State University of Architecture and Civil Engineering, mutual detailed planning of experiement.	Prof. Chang, Ta-Peng
2015/08/06 – 2015/08/26	Theoretical studies, preparation and attendance of The XIth All-	Ivan Popov

	Russian Congress on Basic Problems of Theoretical and Applied Mechanics	
2015/08/19 – 2015/08/26	Attendance of The XIth All-Russian Congress on Basic Problems of Theoretical and Applied Mechanics, Visit Voronezh State University of Architecture and Civil Engineering	Prof. Chang, Ta-Peng
2015/12/21 - 2016/03/04	Experimental results and future plans discussions, writing papers	Ivan Popov

2. Visiting Taiwan from Research Teams working in Russia

Date of Visiting	Main Task and Result	Total member of visiting team/country
2014/05/29 – 2014/06/10	Mutual discussion about the project plans and attendance of conference ICAE 2014.	Prof. Shitikova Marina V., Professor Rossikhin Yurii A.
2016/07/01 – 2016/07/16	Mutual discussion about the project results and future plans	Prof. Shitikova Marina V., Professor Rossikhin Yurii A.

Appendix 3

V. Pattern of Cooperative Research

- Data collection sharing

- Research information exchange

- ☐ Model of theory establishment and inspection
- ☐ Data induction or deduction
- ☐ Device or product design
- ☐ Others (please specify) _____